

Scale Dependence of Nucleon-Nucleon Potentials

Omar Benhar*

INFN and Dipartimento di Fisica, "Sapienza" Università di Roma, I-00185 Roma, Italy

(Dated: March 28, 2019)

The scale-dependence of the nucleon-nucleon interaction, which in recent years has been extensively analysed within the context of chiral effective field theory, is, in fact, inherent in any potential models constrained by a fit to scattering data. A comparison between a purely phenomenological potential and local interactions derived from chiral effective field theory suggests that—thanks to the ability to describe nucleon-nucleon scattering at higher energies, as well as the deuteron momentum distribution extracted from electro-disintegration data—phenomenological potentials are best suited for the description of nuclear dynamics at the scale relevant to neutron star matter.

PACS numbers: 13.75.Cs, 21.30.-x, 21.65.-f

The interpretation of the observed properties of nuclear systems in terms of forces acting between the constituent nucleons has long been recognised as a formidable endeavor. Over six decades after publication of the article in which Hans Bethe famously addressed the question "What Holds the Nucleus Together?" [1], a large amount of work is still being devoted to the development of accurate theoretical models of nuclear forces. Ideally, such models should provide the basis for a unified description of a broad range of systems, from the deuteron to neutron stars [2], in which nucleon-nucleon interactions occur at different ranges, and therefore involve different energies.

In principle, the description of nuclear dynamics should be based on the fundamental theory of strong interactions: Quantum Chromo-Dynamics, or QCD. The efforts aimed at deriving the nucleon-nucleon (NN) potential from lattice QCD have recently achieved remarkable success in predicting its prominent qualitative features [3, 4]. However, the results of pioneering calculations, performed using potentials obtained from lattice QCD studies, suggest that significant developments will be necessary to explain nuclear matter properties at quantitative level [5].

In the absence of a truly fundamental approach, a number of NN potential models have been developed combining the time-honored Yukawa's pion-exchange theory [6]—which is known to describe the interaction at long distance—and phenomenology. In this context, a great deal of empirical information is provided by the two-nucleon system, in both bound and scattering states. Deuteron properties and the large database of NN scattering phase shifts at laboratory energies up to pion production threshold have been extensively exploited to obtain high-precision phenomenological potentials, see Ref. [7] and references therein.

A more fundamental approach, in which the nuclear potential is derived from an effective Lagrangian involving pions and low-momentum nucleons, constrained by

the broken chiral symmetry of QCD, was proposed by Steven Weinberg at the beginning of the 1990s [8]. This formalism provides a systematic scheme, referred to as Chiral Effective Field Theory (χ EFT), in which nuclear interactions are expanded in powers of a small parameter, e.g. the ratio between the pion mass, m_π , or a typical nucleon momentum, Q , and the scale of chiral symmetry breaking, $\Lambda_\chi \sim 1$ GeV. Within this framework, long- and intermediate-range nuclear forces, originating from pion exchange processes, are fully determined by pion-nucleon observables, whereas short-range interactions are described by contact terms involving a set of additional parameters, fixed in such a way as to reproduce NN scattering phase shifts. As pointed out in Ref. [8], a major advantage of χ EFT lies in the possibility to describe two- and many-nucleon potentials within a unified formalism.

In this paper, I will focus on the two-nucleon sector, and compare a phenomenological potential to local χ EFT interactions, to determine their respective ability to describe nuclear matter at supra-nuclear densities and, more generally, short-range nuclear dynamics. This feature is essential to neutron-star modelling, and will be of paramount importance in the dawning era of gravitational wave astronomy [9, 10].

Purely phenomenological potentials such as the Argonne v_{18} model (AV18) [7], widely employed to perform nuclear matter calculations [11, 12], are defined in coordinate space in the form

$$v_{ij} = \sum_{p=1}^{18} v^p(r_{ij}) O_{ij}^p. \quad (1)$$

The functions v^p , involving a set of adjustable parameters whose value is determined fitting NN data, only depend on the distance between the interacting particles, $r_{ij} = |\mathbf{r}_i - \mathbf{r}_j|$. The operators O_{ij}^p , on the other hand, account for the strong spin-isospin dependence of NN interactions, as well as for the presence of non-central forces. The dominant contributions to the sum appearing in the right-hand side of Eq.(1) are those associated with the six operators

$$O_{ij}^{p \leq 6} = [\mathbb{1}, (\boldsymbol{\sigma}_i \cdot \boldsymbol{\sigma}_j), S_{ij}] \otimes [\mathbb{1}, (\boldsymbol{\tau}_i \cdot \boldsymbol{\tau}_j)], \quad (2)$$

* omar.benhar@roma1.infn.it

where the Pauli matrices σ_i and τ_i describe spin and isospin of the i -th nucleon, respectively, and $S_{ij} = 3(\mathbf{r}_{ij} \cdot \sigma_i)(\mathbf{r}_{ij} \cdot \sigma_j)/r_{ij}^2 - (\sigma_i \cdot \sigma_j)$. The contributions corresponding to $p = 7, \dots, 14$ are associated with the non-static components of the NN interaction, while those corresponding to $p = 15, \dots, 18$ take into account small violations of charge independence. For large distances the AV18 model reduces to Yukawa's one-pion-exchange potential, that can be written in terms of the six operators of Eq.(2).

At leading order (LO) of χ EFT, the NN potential comprises Yukawa's one-pion exchange and two contact terms. Next-to-leading order (NLO) and next-to-next-to-leading order (N²LO) contributions also involve two-pion exchange, as well as a set of additional contact terms.

Early χ EFT potentials have been derived in momentum space [13, 14]. A procedure to obtain a local coordinate space representation—needed to carry out accurate Quantum Monte Carlo (QMC) calculations—has been developed in Refs. [15, 16]. The numerical results of calculations performed using the Auxiliary Field Diffusion Monte Carlo (AFDMC) technique demonstrate that N²LO coordinate space Hamiltonians including both two- and three-nucleon interactions provide a remarkably good account of the ground-state energies and charge radii of nuclei with $A \leq 16$ [17].

Theoretical studies based on χ EFT have been also extended to nuclear matter [16, 18]. However, the present development of the QMC approach, recently reviewed in Ref. [19], only allows to treat pure neutron matter (PNM). Combined analyses of PNM and isospin-symmetric nuclear matter (SNM)—needed to study the properties of β -stable neutron star matter—have been carried out within the framework of more approximated methods [20].

Being based on a low momentum expansion, χ EFT is inherently limited when it comes to describing dense systems, in which short-range dynamics plays a dominant role and NN interactions involve high energies. In addition, chiral potentials depend on a momentum-space cutoff, Λ , which in the coordinate-space representation is replaced by a parameter, R_0 , determining the range of the regulator function that smoothly cuts off one- and two-pion exchange interactions at short distances. In Refs. [15, 16], the same range, $R_0 \sim 1$ fm, corresponding to $\Lambda \sim 500$ MeV, has been also used to smear the δ -functions arising from Fourier transformation of the contact terms. As a result, χ EFT potentials are expected to describe interactions up to an energy scale—or, equivalently, down to a resolution scale—determined by the combined effects of the truncation of the low-momentum expansion and the range of the regulator function.

The scale dependence, which naturally emerges within the context of χ EFT, is also inherent in any phenomenological models of the NN potential obtained from a fit to scattering data. Because the fit actually involves the scattering amplitude, which is explicitly energy depen-

dent, in this case the scale is simply determined by the upper limit of the energy range in which the data can be accurately reproduced. Note that this conclusion applies to purely phenomenological and χ EFT potentials alike.

In view of the above considerations, the questions arise of what the energy scale relevant to neutron star matter is, and what potential model is best suited to describe the corresponding regime. To address these issues, consider that in strongly degenerate fermion systems, such as cold nuclear matter, only nucleons in states close to the Fermi surface can participate in scattering processes. It follows that the center-of-mass energy of the collisions can be written in terms of the nucleon Fermi momentum, which in turn is simply related to the density. In the case of head-on collisions in PNM at density n one finds

$$E_{\text{cm}} = \frac{1}{m}(3\pi^2 n)^{2/3}, \quad (3)$$

where m is the nucleon mass.

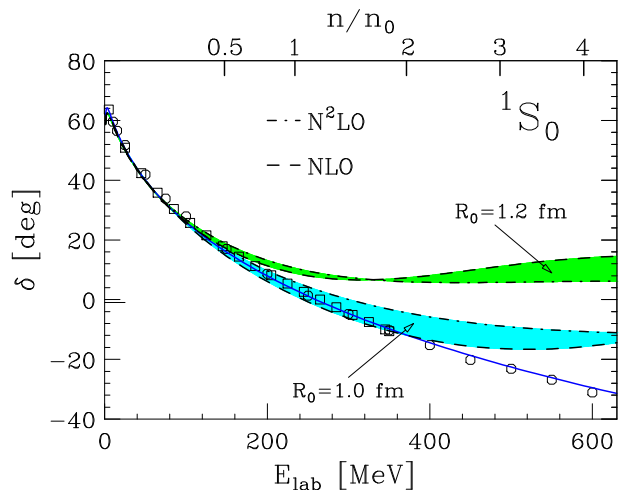


FIG. 1. Neutron-proton scattering phase shifts in the 1S_0 channel, as a function of kinetic energy of the beam particle in the laboratory frame (bottom axis). The corresponding density of PNM—in units of the equilibrium density of SNM, $n_0 = 0.16 \text{ fm}^{-3}$ —is given in the top axis. The solid line has been obtained using the AV18 potential, while the shaded regions illustrate the spread between the NLO (dashed lines) and N²LO (dot-dash lines) predictions of the χ EFT potentials of Ref. [16], obtained setting $R_0 = 1.0$ and 1.2 fm. Squares and circles represent the results of the analyses of Refs. [22, 23] and [24], respectively.

Figure 1 shows the energy dependence of the proton-neutron scattering phase shifts in the 1S_0 partial wave, obtained within the approach of Ref. [21] using the AV18 potential and the local chiral potentials of Ref. [16]. Note that the AV18 interaction has been obtained fitting all phase shifts included in the Nijmegen data base, extending up to $E_{\text{lab}} = 350$ MeV, while the fit performed by the authors of Ref. [16] is limited to $E_{\text{lab}} = 150$ MeV and 100 MeV for $R_0 = 1.0$ and 1.2 fm, respectively.

The solid line represents the results obtained using the AV18 potential, while the shaded regions illustrate the

spread between the NLO (dashed lines) and N²LO (dot-dash lines) χ EFT predictions corresponding to $R_0 = 1.0$ and 1.2 fm. It is apparent that the uncertainty associated with the cutoff R_0 is larger than the one arising from the convergence of the chiral expansion, and that the results obtained with the choice $R_0 = 1$ fm, leading to a harder interaction, provide a better description of the phase shifts at energies larger than ~ 150 MeV. However, in this case the dashed line, showing the results of the NLO approximation, turns out to lie consistently closer to the data than the dot-dash line, corresponding to the N²LO approximation.

The top axis of Fig.1 reports the values of PNM density, obtained from Eq. (3) with $E_{\text{lab}} = 2E_{\text{cm}}$, in units of the equilibrium density of SNM, $n_0 = 0.16 \text{ fm}^{-3}$. The AV18 potential, yielding an accurate description of the data up to energies $E_{\text{lab}} \approx 600$ MeV—well beyond pion production threshold—appears to be best suited to describe matter at densities as high as $4n_0$, while the region of applicability of the potentials of Ref. [16] is much more limited. The picture emerging from Fig. 1 is consistent with the results of Ref. [18], whose authors conclude that using interactions obtained from χ EFT the equation of state of PNM can only be reliably calculated up to $n \lesssim 2n_0$.

The accuracy to which a potential describes short-range interactions, involving large energies, can be further investigated in the two-nucleon sector, studying observables that carry information on the high-momentum components of the deuteron wave function.

Up to corrections arising from final state interactions and two-body current contributions, which can be accurately taken into account, the measured cross section of the deuteron electro-disintegration process

$$e + {}^2\text{H} \rightarrow e' + p + n, \quad (4)$$

in which the scattered electron and the knocked-out proton are detected in coincidence, provides a measurement of the momentum distribution

$$n(k) = \left| \int d^3r e^{i\mathbf{k}\cdot\mathbf{r}} \psi_D(\mathbf{r}) \right|^2, \quad (5)$$

where $\psi_D(\mathbf{r})$ denotes the deuteron wave function, for $k \lesssim 300$ MeV [25, 26].

Additional information on $n(k)$ is obtained from the cross section of the inclusive reaction, in which only the scattered electron is detected [27]. The observation of scaling in the variable y , defined by the relation

$$\omega + M_D = \sqrt{m^2 + (q + y)^2} + \sqrt{m^2 + y^2}, \quad (6)$$

where M_D is the deuteron mass and q and ω denote the momentum and energy transfer, respectively, reflects the onset of the kinematical regime in which quasi-elastic nucleon knockout is the dominant process contributing to the cross section. In this region the electromagnetic response of the target nucleus, which in general depends on

both q and ω , becomes a function of the single variable $y = y(q, \omega)$, which is simply related to the initial momentum of the struck nucleon, and $n(k)$ can be obtained from inclusive data. The analysis carried out by the authors of Ref. [28], based on the cross sections reported in Refs. [29, 30], provides an accurate determination of $n(k)$ for momenta as high as 700 MeV. High-momentum components have been shown to strongly affect the inclusive electron-deuteron cross section in the kinematical region of high q and $\omega \ll \sqrt{q^2 + m^2} - m$, corresponding to large negative values of y [31].

In Fig. 2 the deuteron momentum distributions obtained from the AV18 potential and the chiral potentials of Ref. [16] are compared to the available data. Open circles and squares correspond to the analyses of the measured ${}^2\text{H}(e, e'p)$ [25] and ${}^2\text{H}(e, e')$ [29, 30] cross sections carried out by the authors of Refs. [26] and [28], respectively. It has to be emphasized that the excellent agreement between the results of Refs. [26] and [28] at $k \lesssim 300$ MeV strongly supports the validity and accuracy of the y -scaling analysis.

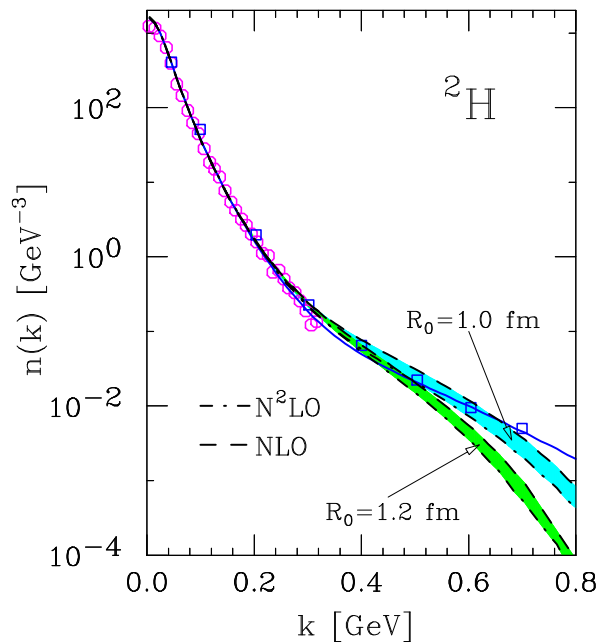


FIG. 2. Deuteron momentum distribution. The solid line has been obtained using the AV18 potential, while the shaded regions illustrate the spread between the NLO (dashed lines) and N²LO (dot-dash lines) predictions of the χ EFT potentials of Ref. [16], obtained setting the parameter R_0 to 1.0 and 1.2 fm. Open circles and squares represent the results of the analyses of electron scattering data carried out by the authors of Refs. [26] and [28], respectively.

The pattern emerging from Fig. 2 appears to be consistent with that of Fig. 1. The phenomenological AV18 potential accounts for the data up to the highest momentum, while the chiral interactions provide an accurate description only at $k \lesssim 300$ MeV. At higher momentum, the results obtained using the harder potentials, correspond-

ing to $R_0 = 1$ fm, are generally closer to the data, but the uncertainty associated with the truncation of the low-momentum expansion rapidly increases, reaching $\sim 50\%$ at $k \sim 500$ MeV. At $k \gtrsim 600$ MeV the predictions of χ EFT tend to fall well below the experimental points, irrespective of the value of R_0 , with the disturbing feature that going from NLO to N²LO leads to a sizable reduction of $n(k)$. To make a connection between the results of Fig. 2 and nuclear matter properties, consider that a Fermi momentum of ~ 300 MeV corresponds to a density $n \sim 0.75 n_0$ in PNM.

Note that, while accounting for only few percent of the wave-function normalisation, high-momentum components sizeably affect the expectation value of the kinetic energy, $\langle T \rangle$. For example, in the case of the AV18 potential, the region of $k > 350$ MeV provides about 16% of the total. Because NN potentials are optimised to reproduce the deuteron ground state energy, $\langle E \rangle$, the availability of a momentum distribution providing an accurate description of the data allows for an independent determination of $\langle T \rangle$, which can be exploited to pin down the expectation value of the interaction energy, $\langle V \rangle$. The values of $\langle E \rangle$, $\langle T \rangle$, and $\langle V \rangle$ obtained using the AV18 potential and the local χ EFT potentials of Ref. [16] are listed in Table I. It is apparent that significant differences occur also at the level of average ground state properties.

	$\langle E \rangle$	$\langle T \rangle$	$\langle V \rangle$
AV18	-2.225	19.791	-22.016
$R_0 = 1.0$ fm LO	-2.019	17.430	-19.449
NLO	-2.150	20.867	-23.017
N ² LO	-2.203	17.640	-19.843
$R_0 = 1.2$ fm LO	-2.025	15.434	-17.459
NLO	-2.162	16.980	-19.142
N ² LO	-2.200	15.546	-17.746

TABLE I. Breakdown of the deuteron binding energy, $\langle E \rangle$, into kinetic and interaction contributions, denoted $\langle T \rangle$ and $\langle V \rangle$, respectively. All energies are given in units of MeV.

The results discussed in this paper show that, unlike phenomenological models, local potentials derived from χ EFT at N²LO level fail to provide an accurate description of NN interactions—both in free space and in the deuteron—at a scale corresponding to center-of-mass energies exceeding ~ 100 MeV. As a consequence, phenomenological models appear to be best suited to study the properties of dense matter relevant to astrophysical applications—such as the equation of state and the dynamical quantities driving neutron-star evolution and gravitational-wave emission [32, 33]—as well as nuclear observables sensitive to short-range dynamics [34, 35].

In principle, the ability of χ EFT potentials to describe nuclear interactions at higher energies can be systematically improved taking into account higher order terms of the chiral expansion. However, the results of the state-of-the-art study of Ref. [36] indicate that including con-

tributions up to N⁴LO does not dramatically change the picture. The region in which the data is accurately reproduced turns out to be extended to $E_{\text{lab}} \sim 300$ MeV, corresponding to densities $n \sim 1.5 n_0$ in PNM, see Fig.1.

Harder χ EFT potentials, suitable to describe dense matter, may be also obtained increasing the value of the cutoff Λ , or, equivalently, reducing the range of the regulator function in coordinate space, R_0 . However, the authors of Ref. [16] report that fitting the NN phase shifts with $R_0 = 0.9$ fm leads to unnatural values of the couplings associated with contact terms. In addition, the results of the phase-shift analysis of Ref. [37], carried out within the infinite-cutoff renormalisation scheme including terms up to N³LO, show that, while in low angular momentum partial waves cutoff independence is achieved at all orders of the chiral expansion for $\Lambda \gtrsim 5$ GeV, the expansion does not converge or fails to converge to the experimental data.

In the absence of a systematic scheme, the uncertainty associated with the phenomenological approach can be estimated comparing results obtained from different potentials providing comparable fits of the data, along the line of the work of Ref. [38]. The results of this study show that the discrepancy between the interaction energies of PNM obtained using the Argonne v_{14} [39] and Urbana v_{14} [40] NN potentials is $\sim 3\%$ at $n \sim n_0$, and remains $\lesssim 20\%$ up to densities $n \gtrsim 3n_0$.

As a final remark, it must be pointed out that the discussion on the scale dependence of nuclear potentials ultimately brings us to the deeper question about the limits of the paradigm underlying nuclear many-body theory. The description in terms of point-like nucleons is expected to break down in the neutron star core [41], as well as in scattering processes involving strongly correlated nucleons [42, 43]. However, the occurrence of y -scaling in electron scattering off a variety of targets, ranging from ²H to nuclei as heavy as ¹⁹⁷Au [44], unambiguously shows that at momentum transfer $q \gtrsim 1$ GeV and negative y the beam particles couple to nucleons, carrying momenta up to ~ 700 MeV. This observation appears to be supported by the results of a simple model calculation of the properties of the six-quark system [45], suggesting that even in the presence of a significant overlap between nucleons the internal quark structure remains largely unchanged. As a consequence, quantitative studies of the transition to the regime in which degrees of freedom other than nucleons become relevant will require the use of NN interaction models suitable to describe nuclear dynamics up to the scale typical of the phenomenological approach.

This contents of this paper largely reflect the views expressed in a talk given by the author at the Workshop *Strong Interaction: From Quarks and Gluons to Nuclei and Stars*, held in Erice, Sicily, in September 2018. The kind hospitality of the Ettore Majorana Foundation and Centre for Scientific Culture is gratefully acknowledged. Thanks are also due to A. Lovato, A. Polls, J. Wambach and R.B. Wiringa for their critical reading of the manuscript.

-
- [1] H.A. Bethe, Scientific American **189**, 58 (1953).
- [2] R.B. Wiringa, Rev. Mod. Phys. **65**, 231 (1993).
- [3] N. Ishii, S. Aoki, and T. Hatsuda, Phys. Rev. Lett. **99**, 022001 (2007).
- [4] S. Aoki *et al* (HAL QCD Collaboration), PTEP **2012**, 01A105 (2012).
- [5] J. Hu, H. Toki, and H. Shen, Scientific Reports **6**, 35590 (2016).
- [6] H. Yukawa, Proc. Phys. Math. Soc. Jpn. **17**, 48 (1935).
- [7] R.B. Wiringa, V.G.J. Stoks, and R. Schiavilla, Phys. Rev. C **51**, 38 (1995).
- [8] S. Weinberg, Phys. Lett. B, **251**, 288 (1990).
- [9] B.P. Abbott *et al* (LIGO Scientific Collaboration and Virgo Collaboration) Phys. Rev. Lett. **119**, 161101 (2017).
- [10] B.P. Abbott *et al* (The LIGO Scientific Collaboration and the Virgo Collaboration) Phys. Rev. Lett. **121**, 161101 (2018).
- [11] A. Akmal and V.R. Pandharipande, Phys. Rev. C **56**, 2261 (1997).
- [12] A. Akmal, V.R. Pandharipande, and D.G. Ravenhall, Phys. Rev. C **58**, 1804 (1998).
- [13] E. Epelbaum, H.W. Hammer, and U.G. Meißner, Rev. Mod. Phys. **81**, 1773 (2009).
- [14] R. Machleidt, and D.R. Entem, Phys. Rep. **503**, 1 (2011).
- [15] A. Gezerlis *et al*, Phys. Rev. Lett. **111**, 032501 (2013).
- [16] A. Gezerlis *et al*, Phys. Rev. C **90**, 054323 (2014).
- [17] D. Lonardonì *et al*, Phys. Rev. Lett. **120**, 122502 (2018).
- [18] I. Tews, J. Carlson, S. Gandolfi, and S. Reddy, ApJ **860**, 149 (2018).
- [19] J. Carlson *et al*, Rev. Mod. Phys. **87**, 1067 (2015).
- [20] I. Bombaci and D. Logoteta, A&A **609**, A128 (2018).
- [21] F. Calogero and D.G. Ravenhall, Nuovo Cimento **32** 1755 (1964).
- [22] J.R. Bergervoet *et al*, Phys. Rev. C **41**, 1435 (1990).
- [23] V.G.J. Stoks, R. A. M. Klomp, M.C.M. Rentmeester, and J.J. de Swart, Phys. Rev. C **48**, 792 (1993).
- [24] R.L. Workman, W.J. Briscoe, and I.I. Strakovsky, Phys. Rev. C **94**, 065203 (2016).
- [25] M. Bernheim *et al*, Nucl. Phys. A **365**, 349 (1981).
- [26] H. Arenhövel, Nucl. Phys. A **384**, 287 (1982).
- [27] O. Benhar, D. Day and I. Sick, Rev. Mod. Phys. **80**, 189 (2008).
- [28] C. Ciofi degli Atti, E. Pace, and G. Salmè, Phys. Rev. C **36**, 1208 (1987).
- [29] W. Schutz *et al*, Phys. Rev. Lett. **38**, 259 (1977).
- [30] S. Rock *et al*, Phys. Rev. Lett. **49**, 1139 (1982).
- [31] O. Benhar and V.R. Pandharipande, Phys. Rev. C **47**, 2218 (1993).
- [32] O. Benhar and A. Lovato, Phys. Rev. C **96**, 054301 (2017).
- [33] G. Camelio, A. Lovato, L. Gualtieri, O. Benhar, J.A. Pons, and V. Ferrari, Phys. Rev. D **96**, 043015 (2017).
- [34] O. Benhar, S.C. Pieper, and V.R. Pandharipande, Rev. Mod. Phys. **65**, 817 (1993).
- [35] N. Fomin, D. Higinbotham, M. Sargsian, and P. Solvignon, Ann. Rev. Nucl. Part. Sci. **67**, 129 (2017).
- [36] E. Epelbaum, H. Krebs, and U.G. Meißner, Phys. Rev. Lett. **115**, 122301 (2015).
- [37] Ch. Zeoli, R. Machleidt, and D.R. Entem, Few-Body Syst. **54**, 2191 (2013).
- [38] R.B. Wiringa, A. Fabrocini, and V. Fiks, Phys. Rev. C **38** 1010 (1988).
- [39] R.B. Wiringa, R.A. Smith, and T.L. Ainsworth, Phys. Rev. C **29**, 1207 (1984).
- [40] I. E. Lagaris and V.R. Pandharipande, Nucl. Phys. A **359**, 331 (1981).
- [41] G. Baym, T. Hatsuda, T. Kojo, P.D. Powell, Y. Song, and T. Takatsuka, Rep. Prog. Phys. **81**, 056902 (2018).
- [42] N. Fomin, D. Higinbotham, M. Sargsian, and P. Solvignon, Annu. Rev. Nucl. Part. Sci. **67**, 129 (2017).
- [43] B. Schmookler *et al* (The CLAS Collaboration), Nature **566**, 354 (2019).
- [44] J. Arrington *et al*, Phys. Rev. Lett. **82**, 2056 (1999).
- [45] M.W. Paris and V.R. Pandharipande, Phys. Rev. C **62**, 015201 (2000).